

## Morphology and properties of new porous biocomposites based on biogenic hydroxyapatite and synthetic calcium phosphates

*O.Sych, N.Pinchuk, A.Parkhomey, A.Kuda, L.Ivanchenko, V.Skorokhod, O.Vasyukiv\*, O.Getman, Y.Sakka\**

I.Frantsevich Institute for Problems of Materials Science, National Academy of Sciences of Ukraine, 3 Krzhizhanovsky Str., 03142 Kyiv, Ukraine

\*National Institute for Materials Science, 1-1, Namiki, Tsukuba, Ibaraki 305-0044, Japan

*Received May 16, 2007*

The new porous biocomposites have been obtained using calcium phosphates (SCP-glass) synthesized by chemical precipitation and the biogenic hydroxyapatite (BHA-glass) extracted from animal bones. The composites prepared at the same conditions have a density of about 2.78 g/cm<sup>3</sup> (SCP-glass) and 2.92 g/cm<sup>3</sup> (BHA-glass) and show good compression strength of about 127 MPa (SCP-glass) and 98 MPa (BHA-glass). The recrystallization of phosphates in composites due to their liquid phase sintering has been revealed.

Получены новые пористые биокompозиты с использованием фосфатов кальция (СФК-стекло), синтезированных методом химического осаждения, и биогенного гидроксиапатита (БГА-стекло), полученного из костей животных. Композиты, полученные в одинаковых условиях, имеют плотность порядка 2,78 г/см<sup>3</sup> (СФК-стекло) и 2,92 г/см<sup>3</sup> (БГА-стекло) и показывают хорошую прочность на сжатие порядка 127 МПа (СФК-стекло) и 98 МПа (БГА-стекло). Обнаружено явление перекристаллизации фосфатов в композитах вследствие их жидкофазного спекания.

The hydroxyapatite Ca<sub>10</sub>(PO<sub>4</sub>)<sub>6</sub>(OH)<sub>2</sub> (HA) is one of the most promising materials for clinical use due to its high biocompatibility and good bioaffinity that stimulates osteoconductivity and is gradually replaced by the host bone after implantation [1]. In recent years, HA, bioactive glasses, tricalcium phosphate (TCP), HA-zirconia composites and bioactive ceramics-polymer composites have been used widely in the orthopedics field due to their bone-like composition as well as good biological and mechanical performances [2–5]. It has been found that dense HA ceramics with a high mechanical strength has often a low biodegradation. The porous materials based on the HA show

a good biodegradation but low mechanical properties restrict their biomedical applications to few circumstances [6]. Therefore, there is a need to prepare implant materials with combined the high bioactivity with good mechanical properties. Phosphate glasses have been used by some researchers to strengthen the HA ceramics [7–12].

Most authors report the partially transformation of HA to TCP during sintering with glass phase [13–18]. It has been shown in our previous studies that Na<sub>2</sub>O–B<sub>2</sub>O<sub>3</sub>–SiO<sub>2</sub> glasses can be used to strengthen HA and improve its bioactivity [19,20]. The originality of our work consists in using glasses without P<sub>2</sub>O<sub>5</sub> and CaO to prepare the cal-

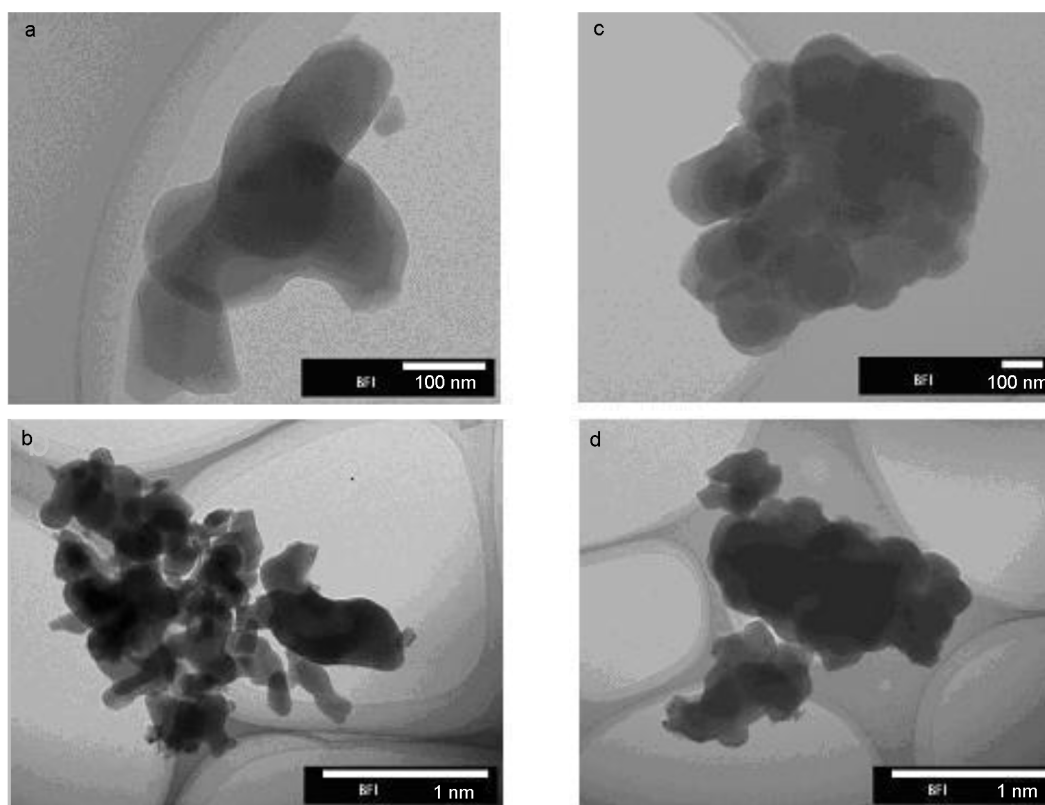


Fig. 1. TEM micrographs of starting SCP (a, b) and BHA (c, d) powders.

cium phosphate composite. Our technology is protected by an Ukrainian Patent [21] and provides the preservation of crystalline phase of calcium phosphate in composites during sintering. For the materials prepared by two-stage sintering, the HA-glass composites show high bioactivity and mechanical strength sufficient for substitution of bone defects [22].

The aim of this work is to obtain new bioactive composite materials based on calcium phosphates — glass phase and to study the morphology, mechanical properties and solubility *in vitro* depending on the type of used phosphates, namely, synthetic calcium phosphates (SCP) and biogenic hydroxyapatite (BHA).

The starting SCP powders were prepared by chemical precipitation from aqueous solution at  $\geq 70^\circ\text{C}$  using calcium nitrate  $\text{Ca}(\text{NO}_3)_2 \cdot 4\text{H}_2\text{O}$  and ammonium phosphate  $\text{NH}_4\text{H}_2\text{PO}_4$  as raw materials. The solution pH was varied between 7–10 using  $\text{NH}_4\text{OH}$ . The reaction mixture was filtered, the precipitate was washed with distilled water, and then dried for 1 h at  $800^\circ\text{C}$ . The starting BHA powders were obtained from animal bones by sintering at  $T \leq 800^\circ\text{C}$ .

The SCP-glass and BHA-glass composites were obtained by two-stage liquid phase sintering under addition of  $\text{Na}_2\text{O}-\text{B}_2\text{O}_3-\text{SiO}_2$  glass components to SCP or BHA powder. The biomaterial initial composition can be presented with the following formula (mol.%):  $45\text{SiO}_2 \cdot 25\text{Na}_2\text{O} \cdot 20\text{B}_2\text{O}_3 \cdot 10$  BHA or SCP.

In the green composites, the particles of glass forming components and both types of phosphate powders have different size achieved maximum  $160 \mu\text{m}$  after sieving. The mixtures of SCP or BHA powder and glass-forming components were pre-sintered at  $1100^\circ\text{C}$  for 15 min. The pre-sintered materials were ground to particle size of  $\leq 160 \mu\text{m}$  and compressed at 150 MPa to form tablets of 15 mm diameter and square blocks of  $4.5 \times 4.5 \times 50.0 \text{ mm}^3$  size. The pressed samples were sintered at  $800^\circ\text{C}$  for 120 min.

The phase compositions of starting SCP and BHA powders and composites were determined by X-ray diffraction analysis (XRD). The transmission electron microscopy (TEM) was used to study the morphology, crystal shape and size of SCP and BHA particles. The scanning electron microscopy

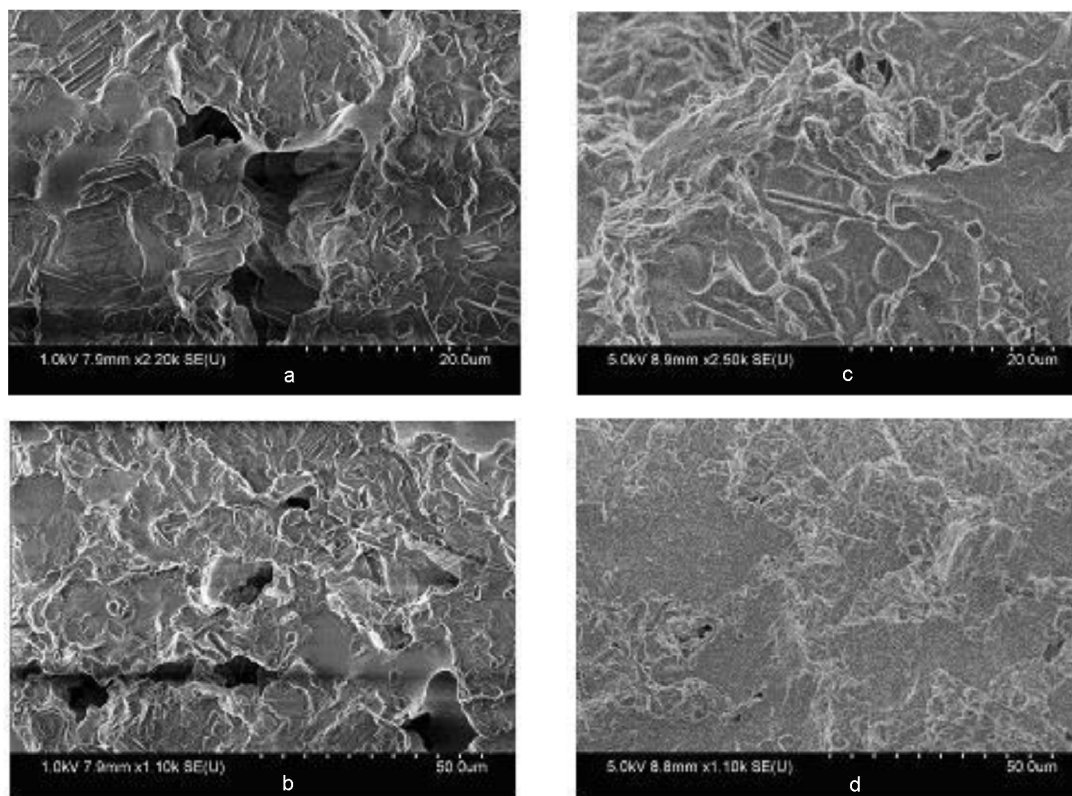


Fig. 2. SEM micrographs of SCP-glass (a, b) and BHA-glass (c, d) composites.

(SEM) was used to examine the surface morphology and element distribution in the structure of the composite samples. The pore and grain sizes were determined using the SEM image analysis software. The density of prepared composites was measured in toluene using the Archimedes principle. The *in vitro* solubility was assessed by soaking composites in physiological solutions for 2, 5, and 7 days at 37°C. The mechanical compression strength was determined on disc-shaped samples and bending strength, on square blocks.

The SCP powders consist of HA,  $\beta$ -tricalcium phosphate (TCP), tetracalcium phosphate (TeCP),  $\beta$ -calcium pyrophosphate (CPP), as determined by XRD. The  $\beta$ -CPP becomes unstable and tends to decompose at the composite sintering temperature, as is confirmed by the IR-spectroscopy results. The SCP and BHA powders morphology presented in Fig. 1 shows crystalline grain aggregates of 205–575 nm size for both phosphate and agglomerates from 0.5 to 160  $\mu\text{m}$  with average grain size of 105–305 nm for SCP and 85–140 nm for BHA powders, which were used to prepare the composite green body.

Fig. 2 shows the SEM surface microphotos of the SCP and BHA composites. It is seen that images of both type of composites exhibit the presence of crystalline blocks (white grains), amorphous glass phase (dark background) and pores (intense dark spots). The computer analysis of the SEM images indicated that average size of crystalline blocks was approximately 0.4–2.2  $\mu\text{m}$  in cross-section and 2.9–7.6  $\mu\text{m}$  in length for the SCP-glass samples and 0.5–1.2 in cross-section 2.1–12.6  $\mu\text{m}$  in length for the BHA-glass samples. Figs. 3a and 3b show the crystalline blocks size distribution for the SCP-glass composite.

The pore size distribution in the SCP-glass and BHA-glass composite samples is presented in Figs. 4a and 4b, respectively. There are some differences in the pore size distribution in both composites. It is seen that the SCP-glass composites have two maxima of the pore size distribution while the BHA-glass composites, only one. The total pore volume determined for this pore sizes is 3 % that is only a small fraction of the total composite porosity calculated from bottle and apparent densities. The bottle density of those SCP-glass and BHA-glass composites is 2.78 and 2.92  $\text{g}/\text{cm}^3$ , respec-

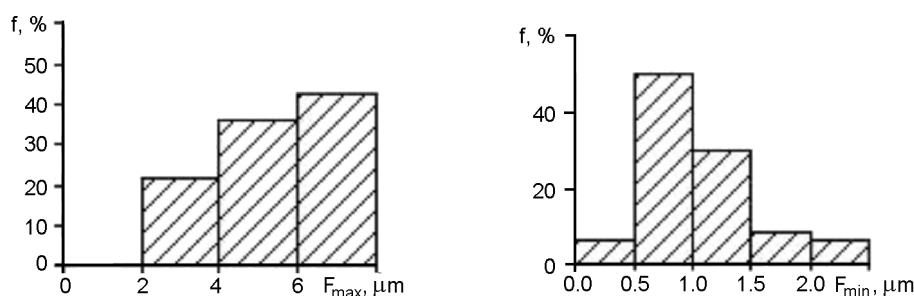


Fig. 3. The length (a) and the cross-section (b) distribution of crystalline blocks in SCP-glass composite ( $\times 2,200$ ).

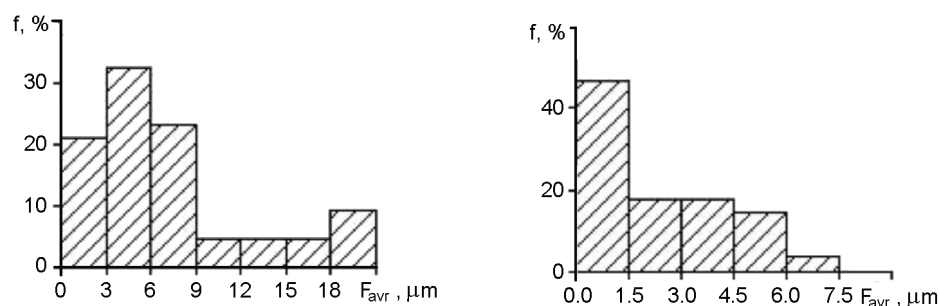


Fig. 4. The pore size distribution in SCP-glass (a) and BHA-glass (b) composite samples ( $\times 500$ , 1100 and 2200 for a;  $\times 2200$  and 6000 for b).

tively, as measured using the Archimedes principle. By comparison of those values with the composite apparent density, the maximum sample porosity was determined presented in Table.

Thus, it is the presence of  $>20 \mu\text{m}$  wide pores (SCP) and  $>7.5 \mu\text{m}$  ones (BHA) that provides in part the total porosity of the studied materials. In our previous studies of composites, it has been established that three main pore groups with maximum sizes close to 2, 10 and  $40 \mu\text{m}$  can be distinguished. The maximum pore size in the BHA-glass composites may attain  $270 \mu\text{m}$  [20]. The SCP-glass composites prepared also by two-stage sintering can have large pores of  $240 \mu\text{m}$  average size [19].

In Fig. 5, the *in vitro* examination results are presented. Those have shown that the solubility in physiological solution are different for the two composite types due to their different composition. The SCP-glass composites show a considerably higher solubility than BHA-glass ones prepared in the same conditions. It was established that the biosolubility of SCP-glass composites is higher than that of BHA-glass ones due to considerable higher solubility of their components, in particular, of TCP and TeCP.

Some physical parameters of SCP-glass, BHA-glass and other biomaterials are compared in Table (data taken from [17, 23–29]). The comparison of SCP-glass and BHA-glass composites indicated that the porosity, compression strength thereof are similar. The compression strength of HA-phosphate glass composites with 10 wt.% of HA is presented also in Table [17]. Our BHA-glass and SCP-glass composites show much higher compression strength. It has been established that mechanical strength of SCP-glass composites after immersion in physiological solution for 5 days decreases from 127 to 51 MPa. At the same time, there are no mechanical strength decrease of BHA-glass composites due to considerable lower biosolubility. In [16], the increasing strength of bioactive glass-ceramics after 2 weeks immersion in Tris buffer was established.

The mechanism of BHA-glass composite sintering can be presented as the following stages: a) particles of  $\text{NaHCO}_3$  and  $\text{H}_3\text{BO}_3$  decompose and form with  $\text{SiO}_2$  a liquid glass phase during pre-sintering of freely poured green composites at low heating rate ( $10^\circ/\text{min}$ ) to  $T_1 = 1100^\circ\text{C}$  and holding for 15 min at this temperature. A liquid glass phase can flow into small pores of BHA particles forming aggregates and agglomerates by capillary forces; b) the liquid glass

Table. Porosity and mechanical properties of composite samples

Material	General porosity (%)	Compression strength (MPa)	Bending strength (MPa)
53 wt.% BHA-47 wt.% Na <sub>2</sub> O·B <sub>2</sub> O <sub>3</sub> ·SiO <sub>2</sub> glass	27.2	98	30
53 wt.% SCP-47 wt.% Na <sub>2</sub> O·B <sub>2</sub> O <sub>3</sub> ·SiO <sub>2</sub> glass	30.0	127	19
(46-50) wt.% BHA-(50-54) wt.% Na <sub>2</sub> O·B <sub>2</sub> O <sub>3</sub> ·SiO <sub>2</sub> glass	26.0-29.4	128-140	30-32
(46-50) wt.% SCP-(50-54) wt.% Na <sub>2</sub> O·B <sub>2</sub> O <sub>3</sub> ·SiO <sub>2</sub> glass	25.1-28.3	131-135	23-26
(10-60)wt.% SHA-(40-90) wt.% HC-2A glass	45-78	12.8-18.0	4.7-12.6 [24]
10 wt.% HA-90 wt.% phosphate glass	-	50-84	-
25 wt.% HA-25 wt.% TCP-50 % glass	55-60	17.0	6.4-9.5
(60-70) wt.% HA-(30-40) wt.% wollastonite	40-50	-	15-25
75 wt.% HA-25 wt.% ZrO <sub>2</sub>	97.0-98.5	-	-
70 wt.% HA-25 wt.% ZrO <sub>2</sub> -5 % ZrF <sub>4</sub>	99.2-99.8	-	-
97.5 wt.% HA-2.5 wt.% CaO·P <sub>2</sub> O <sub>5</sub> glass	2.1-24.1	-	-
96 wt.% HA-4 wt.% CaO·P <sub>2</sub> O <sub>5</sub> glass	2.8-26.1	-	-
HA	5-11.7	-	-
HA (grains)	32	-	<25
HA (grains)	<70	-	<48

phase is flowing into small pores of BHA aggregates during secondary sintering of pressed composite blocks. A small BHA particles are "freely" moving at the same time through the liquid glass and "settling" on more large particles with a directed crystalline orientation similar to crystalline BHA grains of the human bone researched by XRD [30]; c) large pores and some pores of medium size are maintained in composites as a result of pore consolidation typical for the liquid phase sintering [31].

The sintering mechanism of SCP-glass composites can be similar to that proposed by us as a model for the liquid phase sintering of the BHA-glass system. But there are some differences: a) large agglomerates of SCP nanograins, in contrast to BHA ones, do not contain inner pores, formed due to a natural origination and removal of organic impurities; b) due to the SCP multiphase composition, it may be more correctly to characterize the type as a single-block recrystallized structure appearing during the secondary sintering in the presence of a liquid glass phase.

However, the crystalline single blocks in both composite types are similar and can present the same type of the recrystallized HA structure.

In this study, results of phosphate recrystallization were obtained for the first time. Until now, nobody has indicated the formation of single-crystalline blocks due to

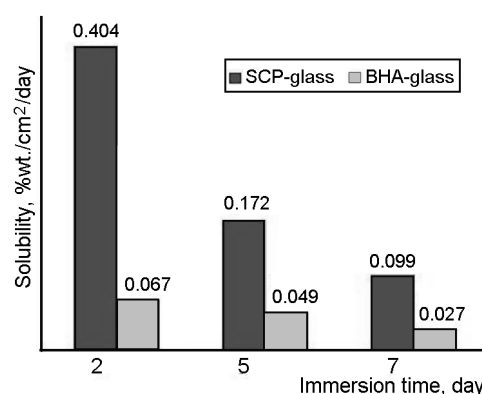


Fig. 5. Dependence of the composite solubility on immersion time in physiologic solution: SCP-glass and BHA-glass.

recrystallization of solid state during liquid phase sintering of a multicomponent system. We have established that the crystalline BHA particles preserve their structure during two-stage sintering, while the SCP particles preserve the structure of their structural components, except for the metastable CPP phase. The indicated recrystallization of solid phase in sintered samples is a factor enhancing the mechanical strength of studied composites.

In this work, the fabrication and study of bioactive calcium phosphate composites is presented. The influence of phosphate type, such as synthetic calcium phosphate and biogenic hydroxyapatite, on the composite

microstructure and main properties are examined. It is shown that formation of the single-block structure during secondary sintering in the presence of liquid glass phase in both composite types can be attributed to the recrystallization of HA structure. The study of properties of prepared SCP-glass and BHA-glass composites makes it possible to expand the range of biocomposites available for use in medicine.

### References

1. T.Kanazawa ed., *Inorganic Phosphate Materials*, Tokyo (1989).
2. N.Pramanik, S.Sasmita, P.Pramanik, P.Bhargava, *J. Am. Ceram. Soc.*, **90**, 369 (2007).
3. S.V.Dorozhkin, *J. Am. Ceram. Soc.*, **90**, 244 (2007).
4. M.Yashima, Y.Kawaike, M.Tanaka, *J. Am. Ceram. Soc.*, **90**, 272 (2007).
5. Manupriya, K.S.Thind, G.Sharma et al., *J. Am. Ceram. Soc.*, **90**, 467 (2007).
6. R.Z.LeGeros, J.P.LeGeros, G.Daculsi et al., in: D.L.Wise, D.J.Trantolo, D.E.Altobelli et al.(Eds.), *Encyclopedic Handbook of Biomaterials and Bioengineering, Part A: Materials*, New York-Basel-Hong Kong (1995), p.1429.
7. J.D.Santos, J.C.Knowles, R.L.Reis et al., *Biomaterials*, **15**, 5 (1994).
8. A.Afonso, J.D.Santos, M.Vasconcelos et al., *J. Mater. Sci. Mater. Med.*, **7**, 507 (1996).
9. J.C.Knowles, S.Talal, J.D.Santos, *Biomaterials*, **17**, 1437 (1996).
10. M.A.Lopes, R.F.Silva, F.J.Monteiro et al., *Biomaterials*, **21**, 749 (2000).
11. A.Yu.Malysheva, B.I.Beletski, E.B.Vlasova, *Glass and Ceramics*, **2**, 28 (2001).
12. M.H.Prado da Silva, A.F.Lemos, J.M.F.Ferreira et al., *Key Eng. Mater.*, **230-232**, 483 (2002).
13. A.F.Lemos, J.D.Santos, J.M.F.Ferreira, *Key Eng. Mater.*, **254-256**, 1033 (2004).
14. Y.Hu, X.Miao, *Ceramics International*, **30**, 1787 (2004).
15. G.Georgiou, J.C.Knowles, J.E.Barralet et al., *J. Mater. Sci. Mater. Med.*, **15**, 705 (2004).
16. D.C.Clupper, J.J.Jr.Mecholsky, G.P.Latorre et al., *J. Biomed. Mater.*, **57**, 532 (2001).
17. F.N.Oktar, G.Goller, *Ceramics International*, **6**, 617 (2002).
18. X.Chatzistavrou, K.Chrissafis, E.Kontonasaki et al., *Key Eng. Mater.*, **2**, 167 (2006).
19. L.A.Ivanchenko, N.D.Pinchuk, A.A.Krupa et al., *Glass and Ceramics*, **60**, 193 (2003).
20. V.V.Skorokhod, L.A.Ivanchenko, N.D.Pinchuk et al., *Functional Materials*, **13**, 260 (2006).
21. Patent of Ukraine No 23250 (1998).
22. L.A.Ivanchenko, V.S.Sulima, N.D.Pinchuk, *Nanostructured Materials and Coatings for Biomedical and Sensor Applications*, **102**, 77 (2003).
23. O.E.Sych, L.A.Ivanchenko, T.I.Fal'kovskaya, *Nanosistemy, Nanomaterial, Nanotehnologii*, **4**, 967 (2007).
24. A.J.Malysheva, B.I.Beleckiy, E.B.Vlasova, *Glass and Ceramics*, **2**, 28 (2001).
25. A.J.Malysheva, B.I.Beleckiy, *Neorg. Mater.*, **2**, 233 (2001).
26. V.V.Shumkova, V.V.Pogrebenkova, V.M.Pogrebenkov, *Keramicheskie Materialy: Proizvodstvo i Primenenie*, **105**, 111 (2003).
27. Z.Evis, R.H.Doremus, *Scr. Mater.*, **56**, 53 (2007).
28. M.A.Lopes, F.J.Monteiro, J.D.Santos, *Biomaterials*, **20**, 2085 (1999).
29. Z.Zyman, V.Filipenko, V.Radchenko et al., *Ortopediya, Travmatologiya i Protezirovaniye*, **1**, 101 (2003).
30. E.P.Podrushnyak, O.N.Lizun, *Vestnik AMN SSSR*, **1**, 37 (1990).
31. V.V.Skorokhod, S.M.Solonin, *Physical and Metallurgical Principles of Powder Sintering*, Metallurgia, Moscow (1984) [in Russian].

## Морфологія та властивості нових пористих біокомпозитів на основі біогенного гідроксиапатиту та синтетичних фосфатів кальцію

**О.Є.Сич, Н.Д.Пінчук, О.Р.Пархомей, О.А.Куда, Л.А.Іванченко, В.В.Скороход, О.О.Васильків, О. І. Гетьман, Ю.Сакка**

Одержано нові пористі біокомпозити з використанням фосфатів кальцію (СФК-скло), синтезованих методом хімічного осадження, та біогенного гідроксиапатиту (БГА-скло), отриманого з кісток тварин. Композити, отримані в однакових умовах, мають густину близько 2,78 г/см<sup>3</sup> (СФК-скло) та 2,92 г/см<sup>3</sup> (БГА-скло), та показують хороші значення міцності на стиск близько 127 МПа (СФК-скло) та 98 МПа (БГА-скло). Виявлено явище перекристалізації фосфатів у композитах внаслідок рідкофазного спікання.